

Spatial distribution and ecological risk assessment of trace metals in urban soils in Wuhan, central China

Chutian Zhang · Yong Yang · Weidong Li ·
Chuanrong Zhang · Ruoxi Zhang · Yang Mei ·
Xiangsen Liao · Yingying Liu

Received: 22 January 2015 / Accepted: 20 July 2015 / Published online: 7 August 2015
© Springer International Publishing Switzerland 2015

Abstract Surface soil samples from 467 sample sites were collected in urban area of Wuhan City in 2013, and total concentrations of five trace metals (Pb, Zn, Cu, Cr, and Cd) were measured. Multivariate and geostatistical analyses showed that concentrations of Pb, Zn, and Cu are higher along Yangtze River in the northern area of Wuhan, gradually decrease from city center to suburbs, and are mainly controlled by anthropogenic activities, while those of Cr and Cd are relatively spatially homogeneous and mainly controlled by soil parent materials. Pb, Zn, Cu, and Cd have generally higher concentrations in roadsides, industrial areas, and residential areas than in school areas, greenbelts, and agricultural areas. Areas with higher road and population densities and longer urban construction history usually have higher trace metal concentrations. According to estimated results of the potential ecological risk index and Nemerow synthesis pollution index, almost the whole urban area of Wuhan is facing considerable potential ecological risk caused by soil trace metals. These results reveal obvious trends of trace metal pollution, and an important impact of

anthropogenic activities on the accumulation of trace metals in soil in Wuhan. Vehicular emission, industrial activities, and household wastes may be the three main sources for trace metal accumulation. Increasing vegetation cover may reduce this threat. It should be pointed out that Cd, which is strongly accumulated in soil, could be the largest soil pollution factor in Wuhan. Effective measures should be taken as soon as possible to deal with Cd enrichment, and other trace metals in soil should also be reduced, so as to protect human health in this important large city.

Keywords Spatial distribution · Risk assessment · Trace metal · Contamination · Urban soil · Wuhan

Introduction

In recent years, with the development of social economy, industrial and economic activities become more concentrated, especially in large cities. Some human activities, such as vehicular emission, industrial and energy production, coal and fuel combustion, construction, and municipal waste disposal, may severely disturb urban soils, giving rise to increasingly serious land contamination and consequently threatening human health (Ljung et al. 2006). Trace metals (i.e., traditionally called “heavy metals”) in soil have some characteristics like ubiquity, toxicity, nonbiodegradation, and long half-lives (Guo et al. 2012), and they can be easily transferred into human bodies through suspended dust inhalation and polluted food ingestion or by direct

C. Zhang · Y. Yang (✉) · R. Zhang · Y. Mei · X. Liao ·
Y. Liu

Key Laboratory of Arable Land Conservation (Middle and Lower Reaches of Yangtze River), Ministry of Agriculture, College of Resources and Environment, Huazhong Agricultural University, Wuhan 430070, China
e-mail: yangyong@mail.hzau.edu.cn

W. Li · C. Zhang
Department of Geography and Center for Environmental Sciences and Engineering, University of Connecticut, Storrs, CT 06269, USA

contact (Benhaddya and Hadjel 2014). Therefore, high concentrations of trace metals in urban soils may pose significant health risks to citizens, particularly children. To make things worse, polluted urban soils may act as the secondary source of trace metals (Cai et al. 2013). On the one hand, soil particles can enter the atmosphere as dusts, being further carried by wind into sensitive environments (Meza-Figueroa et al. 2007). These dusts mainly come from urban construction sites (Zibret 2012) and vehicular exhaust (Johansson et al. 2009). On the other hand, contaminated urban soils may also affect water quality due to surface runoff and soil erosion (Helmreich et al. 2010). Such interaction processes of trace metals with air, soil, and water deteriorate the living environment of humans and further endanger human health. Hence, studying the distribution pattern of trace metals in urban soil and preventing their further accumulation become more and more important.

Urbanization degree may significantly affect the trace metal contamination level of a region (Yang et al. 2014). As the largest developing country in the world, China has experienced a high-speed urbanization and industrialization process in the past decades. Many cities in China are bearing enormous pressure brought by environmental pollution. Therefore, understanding the characteristics of trace metal accumulation in large cities in China is extremely urgent so that suitable prevention measures may be applied quickly and effectively. Wuhan is the largest metropolis in central China, with fast economic growth, high population density, abundant water resources, strong industrial foundation, and highly developed transportation network. Although several studies about trace metals in soil in this city have been done, most of them were restricted to small specific areas (Qu et al. 2013; Yang et al. 2011) or water bodies (Jiang et al. 2014; Liu et al. 2008; Yang et al. 2009, 2010). For example, Qu et al. (2014) recently studied the trace metal contamination status in the Wuhan Donghu High-tech Development Park and assessed the potential ecological risk of trace metals in soil to human health. Therefore, there is a pressing need to study and understand the spatial distribution situation of trace metals in soil in the whole city urban area and further explore the relationships between the urbanization and trace metal accumulation processes in Wuhan.

The main objectives of this study are to (1) measure the current spatial distribution and variability of five trace metals (Pb, Zn, Cu, Cr, and Cd) in top soils in the whole urban area of Wuhan City, (2) assess the

potential ecological risks of trace metals in soil using GIS and some ecological indices, and (3) quantitatively explore the effect of urbanization parameters on trace metal pollution. Such a study will be helpful to evaluating the trace metal contamination situation in the whole city of Wuhan for decision making in environmental planning and remediation and will provide a valuable reference to other large cities with similar urbanization and industrialization situations for environmental management.

Materials and methods

Study area

The Wuhan City is located in the middle reach of Yangtze River. It is the capital of Hubei Province and the largest city in central China, with a population of nearly 10.22 million at the end of 2013 (Wuhan bureau of statistics 2013). About 61 % of Wuhan's population resides in the seven core urban districts (i.e., Jiang'an, Jianghan, Qiaokou, Hanyang, Qingshan, Wuchang, and Hongshan) with an area of 888.42 km² (Wuhan bureau of statistics 2012). Wuhan has a long city history of about 3500 years, traditionally functioning as a military and commercial hub in southern China, and the city landscape has been changing with the changes of dynasties. Water bodies account for nearly a quarter of the total city area. There are hundreds of lakes with various sizes and a couple of large rivers within the administrative borders of the city. Two of the largest urban lakes in China, the Donghu Lake and the Tangsun Lake, are located in Wuhan. Yangtze River, the third largest river in the world, and its largest tributary, Hanjiang River, flow through the center of the city. In addition, Wuhan is also one of China's four major comprehensive transportation hubs. As an industrial city that hosts many heavy industrial enterprises, two state-level economic development parks were established here two decades ago. One of them is the Wuhan Donghu High-tech Development Park, which hosts many photoelectronic and pharmaceutical plants, and the other is the Wuhan Economic & Technological Development Park, which mainly supports automobile and electromechanical plants (see the Wuhan Government webpage, <http://www.wh.gov.cn>).

In this study, a portion of the 3rd Ring Road of Wuhan, a ring expressway, and several low-grade roads were used as the boundaries of the study area, which

covers the seven core urban districts, the southern part of the Caidian district, and the northern part of the Jiangxia district (Fig. 1), with a total area of 1016 km². To explore the relationships between the spatial distributions of soil trace metals and the urbanization in Wuhan, the study area was divided into three regions: (1) R1, the central core urban area, which has a high road density and contains the most prosperous commercial streets (inside the 1st Ring Road); (2) R2, the developed urban area, which covers most of the seven core urban districts (between the 1st Ring Road and the 3rd Ring Road); and (3) R3, the developing urban area, which has a relatively short history of development (outside the 3rd Ring Road, Fig. 1).

Soil sampling and chemical analysis

The study area was divided into grid cells of 1 km × 1 km for sampling so as to reduce the random influence from urban wastes (Rizo et al. 2011). A total of 467 topsoil samples (0~20-cm depth) were collected inside these grid cells in different functional zones (Fig. 1). Among them, 68 were collected from industrial zones (IZ), 92 from roadsides (RS), 109 from residential areas (RA), 27 from school areas (SA), 94 from agricultural areas (AA), and the remaining 77 from greenbelts (GB). At each sample site, three to five subsamples were first collected randomly using a wooden shovel and then mixed together. Nearly 1 kg of the mixed soil sample was selected and stored in a self-sealing plastic bag. All

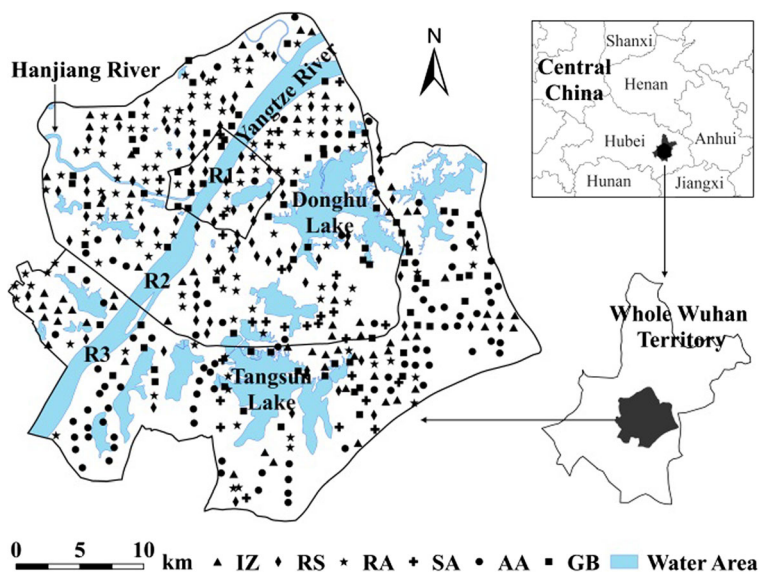
coordinates of the sample sites were recorded using GPS. The soil sampling was conducted in November, 2013.

The samples were air-dried in a laboratory at room temperature, large stones and other debris were removed manually, and then the samples were sieved by a 2-mm polyethylene sieve to remove the rest of the debris, gravel-sized materials, plant roots, and other waste materials. These sieved samples were further ground in an agate grinder, sieved through a 150-µm mesh, and then stored in closed plastic bags for analysis.

For chemical analysis of trace metals, atomic absorption spectrometer (AAS) and inductively coupled plasma atomic emission spectrometry (ICP-AES) are two of the most used traditional methods. High-quality data could usually be obtained by these two methods, but the time and money expenses would be high. Other methods, such as X-ray fluorescence (XRF), are often quicker and less expensive but may not be as accurate as traditional methods. In this paper, both ICP-AES (VISTA-MPX, VARIAN, USA) and XRF (Niton XL2 600, Thermo Scientific, USA) were used in order to get more qualified data in a shorter time with less expense.

The whole set of 467 soil samples was analyzed by XRF, with each soil sample being detected for at least 90 s to ensure data accuracy and all sample measurements being blank-corrected. The relative standard deviations (RSDs) were 1.05~38.07 % for Pb, 1.45~21.44 % for Zn, 6.56~43.58 % for Cu, and 11.74~40.40 % for Cr, respectively. Concentrations of Cd for

Fig. 1 Sampling sites and the division of the study area. IZ, RS, RA, SA, AA, and GB refer to industrial zone, roadside, residential area, schools area, agricultural area, and greenbelt, respectively. The two *black ring lines* represent the 1st Ring Road and the 3rd Ring Road of Wuhan City, respectively



all samples were lower than the detection limit of XRF (25 mg/g) and thus failed to be detected.

Then, 150 soil samples were carefully selected for ICP-AES analysis to shorten analysis time. Most of those selected samples were located in Qingshan district or Donghu High-tech Development Park while the remaining samples were distributed in other districts randomly. About 0.5 g for each selected soil sample was added into 10 mL aqua regia (HCl/HNO₃=3:1). The mixture was then heated on an electric heating plate at 200 °C. After the brown oxynitride vanished, the mixture was cooled to room temperature. Then, the residue was treated with 2 mL perchloric acid and heated until its color turned to gray-white. Finally, the solution was diluted with deionized water and 10 mL digested solution was taken for analyzing total concentrations of Pb, Zn, Cu, Cr, and Cd using ICP-AES. Three duplications were performed for each soil sample, and blank samples were also analyzed. Data quality of ICP-AES and XRF were also verified using previous data (see Appendix 1). All soil samples were analyzed at the Key Laboratory of Arable Land Conservation (Middle and Lower Reaches of Yangtze River), Ministry of Agriculture of China.

Data processing

Although there are totally 467 soil samples, the numbers of measured data used for different soil trace metals in this study are different. They are 360 for Pb, 465 for Zn, 316 for Cu, and 150 for Cr and Cd, respectively. One main reason is that BDLs (measurements of a certain trace metal that are below the corresponding detection limit) of XRF were ignored. According to the results of correlation analysis between ICP-AES and XRF measurements of the 150 selected samples (noted as training samples), concentrations of Pb, Zn, and Cu by XRF at other sampling points were transformed based on the well-fitted regression models, while for Cr and Cd, only their concentrations by ICP-AES were used. Details are given in Appendix 2.

Descriptive statistical analysis, correlation analysis, and ANOVA were carried out using the SPSS software (version 19.0, IBM, USA). Correlations between urbanization indicators and concentrations of Pb, Zn, Cu, Cr, and Cd were assessed using Pearson correlation analysis. The differences in trace metal contents among different functional zones and regions divided by ring roads were investigated using one-way ANOVA analysis. To identify hot spots with high trace metal

concentrations, the spatial distribution maps of trace metals and pollution indices were obtained using ordinary kriging with the help of ArcGIS (version 10.2, ESRI Inc., USA).

Indices for trace metal pollution assessment

To evaluate the contamination levels of studied trace metals (Pb, Zn, Cu, Cr, and Cd), two indices, namely, potential ecological risk index (RI) and Nemeró synthesis pollution index (NPI), were used in this paper. The RI, defined by Hakanson (1980) based on the different toxicities of trace metals and the responses of the environment, is calculated as follows:

$$RI = \sum T_i \frac{C_i}{B_i} \quad (1)$$

where T_i is the toxic response factor of the i th trace metal. According to Hakanson (1980), the toxic response factor values for different trace metal elements are in the order of Zn=1<Cr=2<Cu=Pb=5<Cd=30. C_i is the concentration of the i th trace metal in soil, and B_i is the corresponding reference value of the i th trace metal. In this study, the natural background values of trace metals in Hubei province (China National Environmental Monitoring Centre 1990) were used as their reference values. Four levels of trace metal pollution based on the values of RI are as follows: low potential ecological risk ($RI \leq 150$), moderate potential ecological risk ($150 < RI \leq 300$), considerable potential ecological risk ($300 < RI \leq 600$), and high potential ecological risk ($RI > 600$) (Qu et al. 2014).

The Nemeró synthesis pollution index (NPI) is an integrated index to assess the degree of soil environmental pollution, and the formula is given (Chen et al. 2013) by

$$NPI = \sqrt{\frac{\left(\frac{C_i}{B_i}\right)_{\max}^2 + \left(\frac{C_i}{B_i}\right)_{\text{ave}}^2}{2}} \quad (2)$$

where the meanings of C_i and B_i are the same as those in RI, and the subscripts *max* and *ave* refer to the maximum and average values of C_i/B_i among trace metals for each sample. However, five levels of trace metal pollution are defined based on the values of NPI (Chen et al. 2013), and they are as follows: practically unpolluted ($NPI \leq 0.7$), unpolluted to moderately polluted ($0.7 < NPI \leq 1.0$), moderately polluted ($1.0 < NPI \leq 2.0$),

moderately to strongly polluted ($2.0 < NPI \leq 3.0$), and severely or strongly polluted ($NPI > 3.0$).

Results and discussions

Trace metal concentrations in urban soils

Table 1 lists the statistics of the concentrations of the five trace metals in soil in Wuhan. Compared with the corresponding natural background values in Hubei, Cd shows apparent accumulation, Zn and Pb have the tendency of accumulation, and Cr and Cu averagely do not indicate accumulation. However, the maximum value of Cu is much higher than its corresponding background value, and its coefficient of variation (CV) is much larger than those of other elements, suggesting that Cu may be strongly impacted by human activities and contaminated soils at some places. Moreover, some soil parameters related to trace metal contents were obtained. The urban topsoil pH values of Wuhan City range from 4.9 to 8.9 with a mean value of 6.9 (Gong et al. 2010), indicating that the topsoil in Wuhan City is relatively acidic generally. Soil organic carbon (SOC) contents of industrial zone, roadside, residential area, school area, agricultural area, and greenbelt are 0.38, 0.33, 0.98, 1.28, 0.73, and 0.75 g/kg, respectively (Zhao et al. 2011), implying that SOC content varies significantly among different functional zones. These two soil parameters could help to further understand the spatial distribution patterns of trace metals in Wuhan City.

As shown in Fig. 2, the median concentration values of the studied trace elements are all lower than their corresponding natural background values, except for Cd. However, there are many

outliers with high concentrations of Pb, Zn, and Cu. This means that soils around the sites of these outliers have been severely contaminated by the four trace metals (Pb, Zn, Cu, and Cd). The large CV of Cu also can be explained by the number of extreme values, particularly extremely small values, in measured Cu concentrations.

According to the Chinese Environmental Quality Standards for Soils (State Environmental Protection Administration of China 1995), Pb contents exceed the class I criterion at 18.89 % of sample sites; Zn contents exceed the class I, II, and III criteria at 20.22, 1.72, and 0.22 % of sample sites, respectively; Cu contents exceed the class I and II criteria at 8.23 and 0.95 % of sample sites, respectively; and Cd contents exceed the class III criterion at all sample sites (Table 2). Notably, the four elements of Pb, Zn, Cu, and Cd all exceed the class I criterion at the 11 sample sites that are located in the northeast of the study area. The southern and southeastern winds in summer can carry the emissions from the Qingshan Industrial Zone into this area, and the busy traffic along the Yangtze River may also cause the release of these trace metals in this area.

Comparison of trace metal concentrations in different functional zones

Trace metals in urban soils within different function zones may impose different impacts on human health (Benhaddya and Hadjel 2014). Therefore, soil samples were grouped and their average concentrations for different functional zones were calculated, as shown in Fig. 3. Soils along roadsides have relatively higher contents of Pb, Zn, Cu, and Cd than those in other

Table 1 Summary statistics of soil trace metal concentrations (mg/kg)

Element	N	Minimum	Median	Maximum	Mean	SD	CV (%)	BV	BV-SD
Pb	360	9.17	23.20	143.54	28.16	15.54	55.19	26.70	7.86
Zn	465	19.22	76.66	529.71	88.07	44.93	51.02	83.60	36.15
Cu	316	0.24	15.58	205.38	18.82	17.03	90.47	30.70	14.05
Cr	150	20.06	40.95	75.13	41.85	9.66	23.08	86.00	36.92
Cd	150	0.99	3.16	13.31	3.22	1.21	37.63	0.17	0.19

N number of samples, SD standard deviation, CV coefficient of variation, BV natural background value in Hubei Province (China National Environmental Monitoring Centre 1990), BV-SD standard deviation of natural background value in Hubei

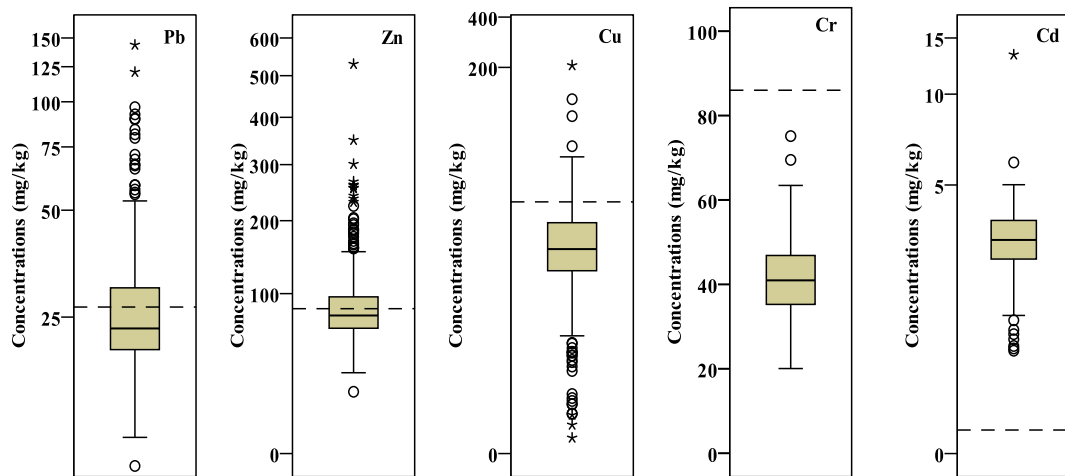


Fig. 2 Box-and-whisker plots for Pb, Zn, Cu, Cr, and Cd with outliers. The horizontal dotted lines represent the natural background values of corresponding trace metals in Hubei

functional zones, followed by those in industrial areas and residential areas. Because roadsides are the areas firstly receiving traffic emissions, high concentrations of Pb, Zn, and Cu in urban soils should be closely related to traffic exhaust. Although leaded gasoline has been banned in China for many years, the long history of widely using leaded gasoline still left much Pb with high concentrations in urban soils. This situation is also related with the long half-life of Pb (Cai et al. 2013). The wear and tear of vehicle over time may be one reason for the accumulation of Zn and Cu in urban soils. Zn compounds are important constituents of lubricating oils, and high vehicle wearing may contribute significantly to the Zn content in urban soils (Helmreich et al. 2010). Cu has been widely used in vehicle braking systems, and frequent brake uses on roads, especially crossroads, can be a major source of Cu in soil (Johansson et al. 2009). This may be why the average

concentration of Cu along roadsides is significantly higher than that in other functional zones (Fig. 3). There is no significant difference between Cr concentrations in different functional zones ($p > 0.05$), indicating that land uses have no strong effect on the distribution of Cr in urban soils.

Moreover, trace metal contents in roadsides, industrial areas, and residential areas are generally higher than their corresponding natural background values, except for Cu and Cr. This indicates that industrial activities (Zheng et al. 2007), municipal waste disposal, and incineration (Anikwe and Nwobodo 2002) and other human activities may be responsible for high trace metal accumulation in those areas, besides vehicular emission. Relatively low average concentrations of Pb, Zn, Cu, and Cd are found in school areas, greenbelts, and agricultural regions. This may result from the high greening rate in these areas and the environmental protection measures taken in recent years. Notably, greenbelts in this paper include green lands, parks, and some other regions covered by large areas of lawn, where some soils have long history but others may be carried in from other places. Therefore, soils in greenbelts may have complex sources. However, the average concentrations of Cd for different functional zones do not vary much. It was reported that irrigations using river water polluted by industries often occurred (Gupta et al. 2010) and phosphate fertilizers containing Cd were widely used (Atafar et al. 2010). These may be the sources of soil Cd contamination in agricultural regions and greenbelts.

Table 2 The quality status of soil samples based on the pollution standards for Pb, Zn, Cu, and Cd according to the Chinese Environmental Quality Standard for Soils (GB 15618–1995)

	Pb	Zn	Cu	Cd
1st standard (mg/kg)	35	100	35	0.2
2nd standard (6.5 < pH < 7.5) (mg/kg)	300	250	100	0.3
3rd standard (mg/kg)	500	500	400	1
Samples \geq 1st standard (%)	18.89	20.22	8.23	100
Samples \geq 2nd standard (%)	0	1.72	0.95	100
Samples \geq 3rd standard (%)	0	0.22	0	100
Total samples	360	465	316	150

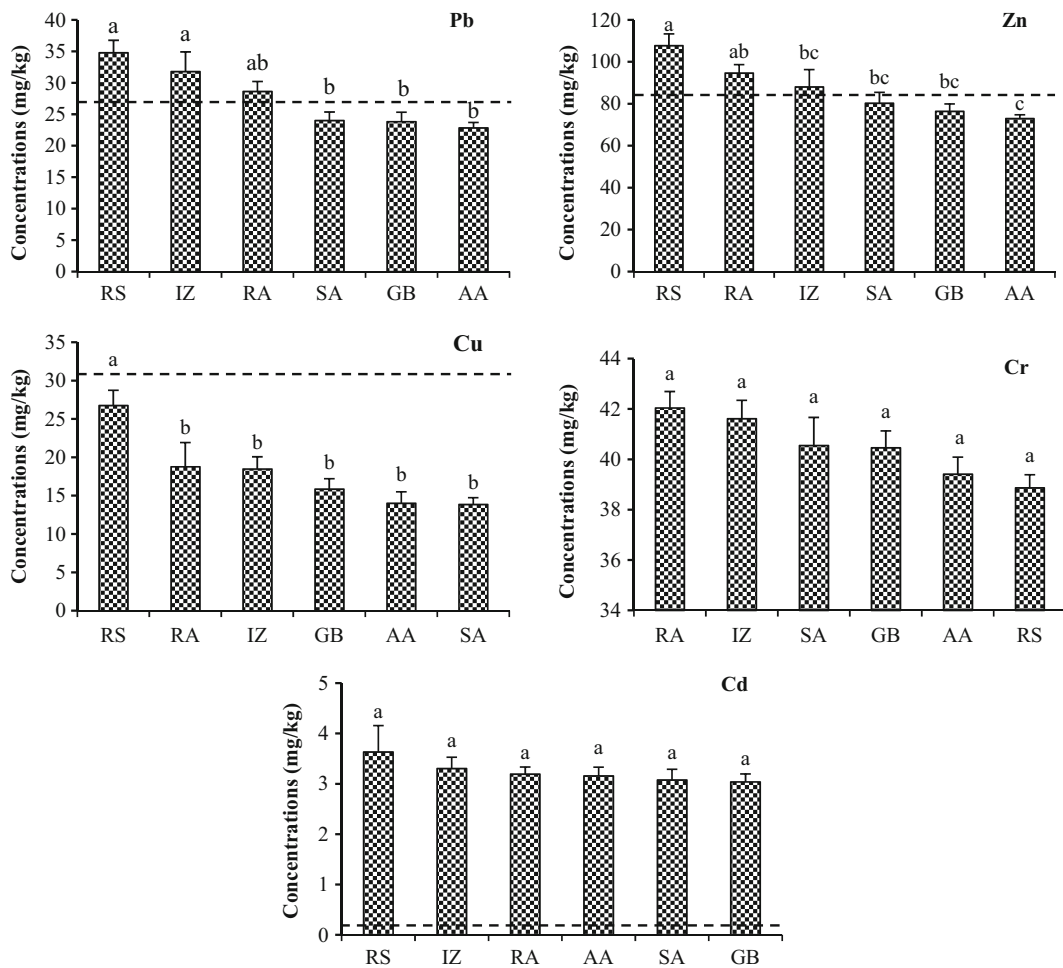


Fig. 3 Mean concentrations with standard errors of trace metals in soil in different functional regions in Wuhan City. IZ, RS, RA, SA, AA, and GB refer to industrial zone, roadside, residential area, school areas, agricultural area, and greenbelt, respectively.

Horizontal dotted lines represent corresponding natural background values in Hubei. Different letters indicate that average metal concentrations in soil in the corresponding functional regions are significantly different ($p < 0.05$)

Table 3 Mean trace metal concentrations (mg/kg) in urban soils in different cities over the world

City	Pb	Zn	Cu	Cr	Cd	References
Wuhan, China	28.16	88.07	18.82	41.85	3.22	This study
Wuhan, China	33	85	34	85	0.20	Gong et al. (2010)
Beijing, China	39.50	89.63	34.42	60.27	0.19	Xia et al. (2011)
Urumqi, China	53.53	294.47	94.54	54.28	1.17	Wei et al. (2009)
Shanghai, China	70.69	301.4	59.25	107.9	0.52	Shi et al. (2008)
Guangzhou, China	65.7	300.7	45.2	26.0	0.6	Cai et al. (2013)
Turku, Finland	20	72.5	19.15	37	0.2	Salonen and Korkka-Niemi (2007)
Guwahati, India	170.5	286	124.4	122.9	18	Mahanta and Bhattacharyya (2011)
Ibadan, Nigeria	95.1	228.6	46.8	64.4	8.4	Odewande and Abimbola (2008)
Berlin, Germany	40.6	101	18.5	18.1	0.5	Birke and Rauch (2000)
Havana, Cuba	56	104	10.3	–	–	Rizo et al. (2011)

Comparison of trace metal concentrations in typical cities around the world

Compared with the reported concentrations of trace metals in urban soils of some typical cities over the world (Table 3), trace metal concentrations in soil of Wuhan are generally lower than those of other cities (but they are comparable to those measured in Turku and Beijing), except for Cd. Concentrations of Pb and Zn in soil in Wuhan are comparable to those in cities such as Berlin and Havana but are much lower than those in Urumqi, Shanghai, Guangzhou, Guwahati, and Ibadan. Concentrations of Cu and Cr in soil in Wuhan are generally lower than those in most of other cities. However, the average concentration of Cd in Wuhan is much higher than that in most of other cities except for Guwahati and Ibadan. This means that the Cd pollution in Wuhan has reached a very serious level. Compared with the previous study about Wuhan City made by Gong et al. (2010), concentrations of Pb and Zn are comparable while concentrations of Cu and Cr are lower and that of Cd is much higher in this study. The differences may be caused by different sampling strategies and measuring methods.

Spatial distributions of trace metals in soil

The spatial distributions of Pb, Zn, Cu, Cr, and Cd in topsoils in the urban area of Wuhan are shown in Fig. 4. In the maps, green means that the metal content is lower than the background value at the place, and the greener the lower; yellow means that the concentration of the trace metal is close to the background value; and red means that the metal content is higher than the background value, and the redder the higher.

The spatial distribution maps of Pb, Zn, and Cu show similar spatial patterns: The concentrations of these three trace metals are relatively high along Yangtze River and decrease gradually with the distance from the river (the city center is along the river). Meanwhile, they are much higher along the northern section of Yangtze River than along the south section. This may be caused by the fact that the development of Wuhan City relied greatly on Yangtze River; thus, human activities tended to be more frequent along this river than in other regions of the city. What's more, large industries have been mainly distributed in the north region along the river. In addition, three hot spot areas can be identified. The first one is located at the center of the central

core urban area. This area is surrounded by the 1st Ring Road of Wuhan City, with lots of people living there and numerous cars going through. The second one is located in the most northern region of the study area, along the banks of Yangtze River. The northern part of this hot spot area was an old industrial base once, and a new industrial park named "Wuhan Dijiao Urban Industrial Park" has been planned to be settled here. This hot spot area is adjacent to the west of the Qingshan Industrial Park, and there are many residential communities within it. The last hot spot area is located between the Donghu Lake and the Yanxi Lake. This area is a part of the famous Qingshan Industrial Park. Many large factories such as Wuhan Heavy Industry Casting & Forging Co., Ltd. and Wuhan Marine Machinery Co., Ltd. are located here. In short, the accumulation of Pb, Zn, and Cu is associated with multiple factors including vehicular emission, industrial activities, and municipal activities.

Cr and Cd have different spatial distribution characteristics compared with other elements. No decreasing trend with the distance from Yangtze River exists. The concentrations of Cr in the whole study area are lower than its natural background value, probably implying that anthropogenic activities have little impact on soil Cr. However, the spatial distribution map of soil Cd for the whole study area is covered by red color, and even the minimum interpolated value (1.36 mg/kg) is seven times higher than the corresponding natural background value (0.17 mg/kg). Previous studies (Yang et al. 2009) also support our result that Cd has a relatively higher concentration in soil in Wuhan. Ma et al. (2005) found that Cd was relatively abundant in the crust rocks of the Yangtze River basin and the Hanjiang River basin, and it tends to enrich in alluvial soils due to its physicochemical properties. Thus, natural factors may be a main source for the relatively high level of Cd concentration in Wuhan City. Still, some industrial discharges from smelting and electric plating may significantly contribute to the wide spreading of Cd in soils in Wuhan (Wei et al. 2009; Yang et al. 2009). In addition, from the spatial distribution maps of Cr and Cd, one can see relative enrichment in the three hot spot areas identified by Pb, Zn, and Cu, compared with other areas.

Urbanization effect

The relationship between the development process of urbanization and trace metal accumulation in urban soils had been discussed in some previous studies

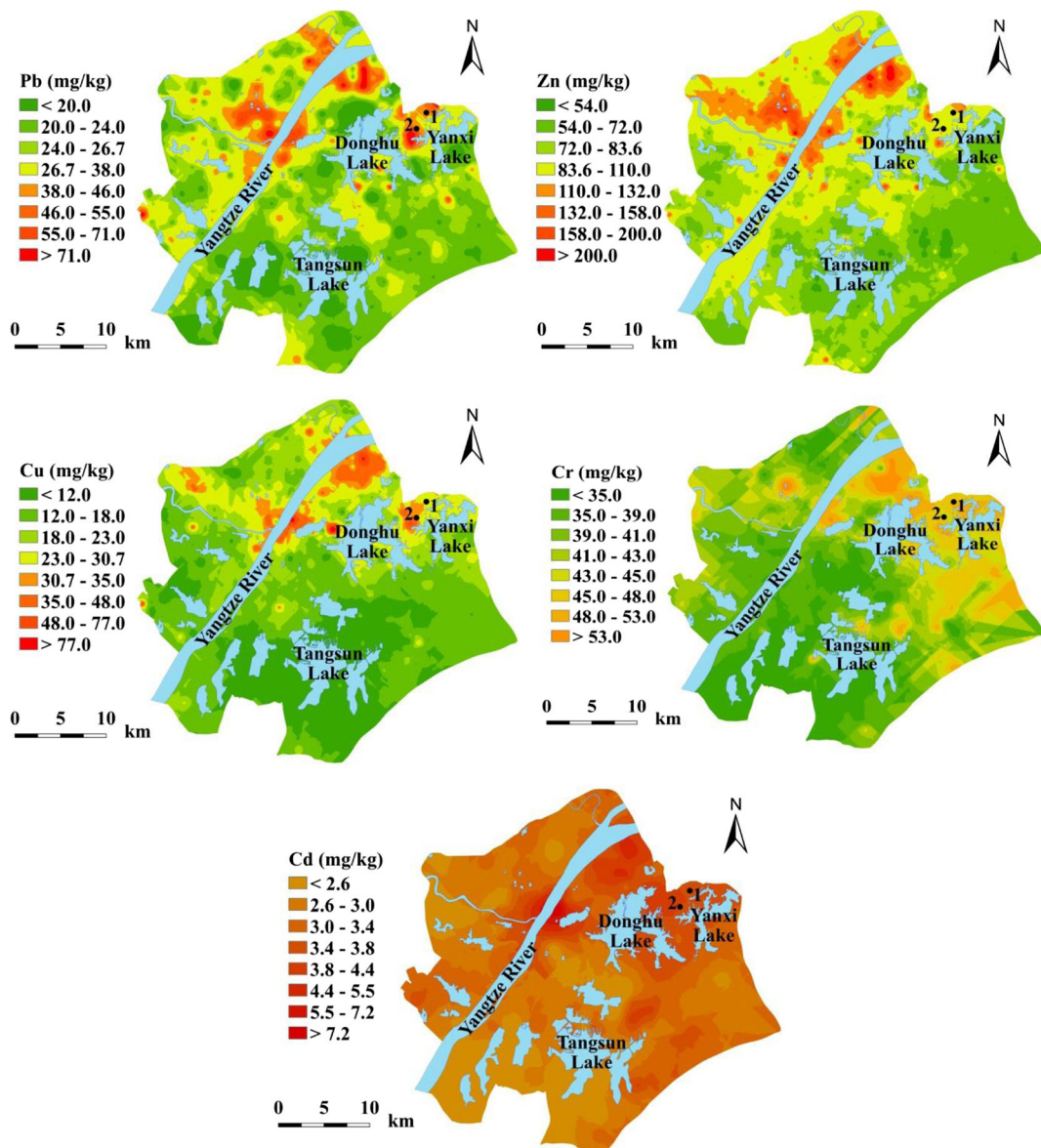


Fig. 4 Spatial distributions of trace metal concentrations in the study area. 1: the location of the Wuhan Heavy Industry Casting & Forging Co., Ltd., 2: the location of the Wuhan Marine Machinery Factory Co., Ltd.

(Yang et al. 2014). In this paper, three urbanization indicators—history of urban construction, weighted road density, and population density—were adopted to quantitatively describe this relationship.

Effect of history of urban construction

Similar to many other big cities, Wuhan developed step-by-step from its center to suburb areas. Therefore, different parts of the study area could well represent the

history of urban construction. The whole study area was divided into three subareas based on the ring roads (Fig. 1). The average concentrations of Pb, Zn, Cu, Cr, and Cd in different subareas with ANOVA results are shown in Fig. 5. These five metals share the same trend in their mean value changing from city center to suburb, that is, R1>R2>R3. While the average contents of Pb, Zn, and Cu are significantly different from R1 to R3 ($p<0.05$), the average contents of Cd for the R2 and R3 have no much difference ($p>0.05$). The common trend

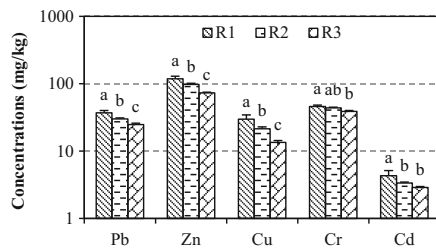


Fig. 5 Average concentrations of trace metals (Pb, Zn, Cu, Cr, and Cd) in soil in three different subareas of the study area. *R1*: the central core urban area (inside the 1st Ring Road). *R2*: the developed urban area (between the 1st Ring Road and the 3rd Ring Road). *R3*: the developing urban area (outside the 3rd Ring Road). Different letters indicate that average metal concentrations in soil in the corresponding subareas are significantly different ($p < 0.05$)

may be due to the fact that trace metals have been accumulated for longer time in older urban areas, which is in agreement with previous studies (Xia et al. 2011).

Effects of weighted road density and population density

Weighted road density is defined as the weighted sum of the lengths of roads (km) per square kilometer (Rose et al. 2009). As shown in Fig. 6, roads in Wuhan's urban area can be classified into three classes: national road, provincial road, and county road. The road data was obtained by digitalizing the transportation map of Wuhan City (1:10,000, published in 2012). The weights for national road (0.3537), provincial road (0.3379), and county road (0.3084), suggested by Liu et al. (2014) based on the traffic volumes of different road classes, were adopted in this study. The 1 km × 1 km population densities data of Wuhan in 2013 was obtained from LandScan (Bright et al. 2013).

As given in Table 4, the concentrations of Pb, Zn, and Cu have significant positive correlations with weighted road density. This further confirms that traffic exhaust is the main source of Pb, Zn, and Cu in urban soils. As to population density, a similar relationship could be detected. Higher population density implies more frequent daily activities, such as the uses of decorations, electronic components, pesticides, and so on (Lin et al. 2002), thus resulting in more trace metals being accumulated in the living environment. Peng et al. (2013) also found that urban areas with higher population densities and larger numbers of vehicles had higher soil trace metal concentrations.

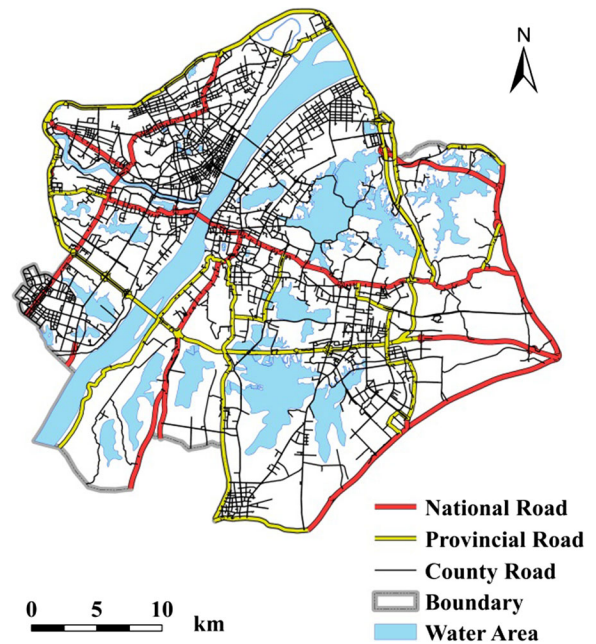


Fig. 6 The network of roads and their classification in the study area

Risk assessment

Because the numbers of samples for Pb, Zn, Cu, Cr, and Cd are different but RI and NPI are both integrated scores of all the studied trace metals, in this study, we used the spatial distribution maps of soil trace metals interpolated by ordinary kriging to calculate the RI and NPI values in the study area. This can ensure that the data of all studied trace metals are available at every location and no further interpolations are necessary for mapping the RI and NPI. Figure 7 provides the RI and NPI maps. From the RI map, one can see that nearly 72.39 % of the study area has reached the level of “considerable potential ecological risk” (i.e., $300 < RI \leq$

Table 4 Pearson correlation coefficients of the average concentrations of trace metals with population density and weighted road density

	Pearson correlation coefficient				
	Pb	Zn	Cu	Cr	Cd
Weighted road density	0.149**	0.199**	0.124*	0.023	0.116
Population density	0.287**	0.380**	0.243**	0.149	0.155

**The correlation is significant at the 0.01 level (two-tailed); *the correlation is significant at the 0.05 level (two-tailed)

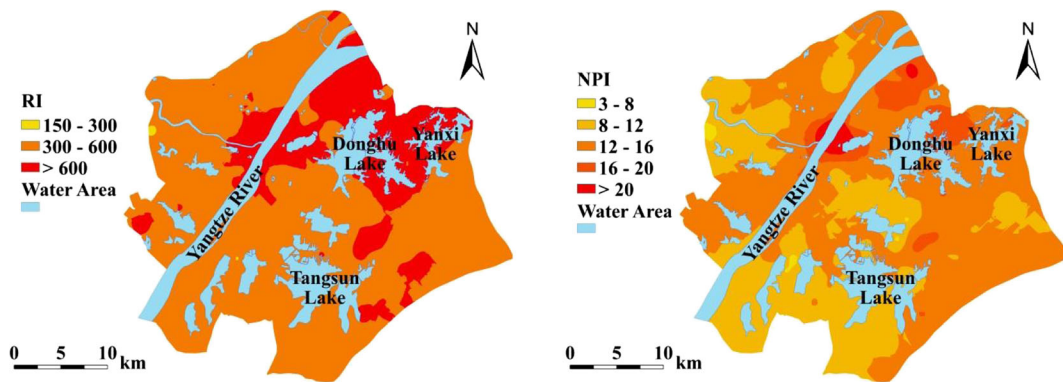


Fig. 7 Spatial distribution maps of the RI and NPI of trace metals in the study area. Note that the NPI legend does not reflect the different pollution levels because the whole area is in the highest level (i.e., >3.0)

600), 27.56 % of the study area reaches the level of “high potential ecological risk,” and only 0.05 % of the study area is in the “moderate potential ecological risk” level. Apparently, the three hot spot areas identified in Fig. 4 for high contents of trace metals (mainly Pb, Zn, and Cu) are identified again in the distribution map of RI. In the spatial distribution map of NPI, it is obvious that the whole study area is within the pollution class of “severely or strongly polluted” (i.e., $NPI > 3.0$). This means that RI is more capable than NPI in representing the pollution risk of trace metals in soil. Therefore, enhanced strategies should be carried out to eventually reduce the accumulated trace metal contents from urban soil in Wuhan.

Conclusions

This investigation of soil trace metals for the urban area of Wuhan City revealed clear spatial patterns of the five trace metals (Pb, Zn, Cu, Cr, and Cd). Some sample sites have higher concentrations of Pb, Zn, and Cu, coupled with large coefficients of variation (especially for Cu), than the corresponding natural background values of Hubei Province, indicating the strong impact of human activities on the accumulation of these trace metals in soil. What is more, Pb, Zn, and Cu share similar spatial patterns that their concentrations are higher along Yangtze River in the northern area of the city and gradually decrease from city center to suburbs. On the contrary, Cr and Cd are relatively spatially homogenous with low coefficients of variation, suggesting that their major source maybe natural soil parent materials. The content of Cd is higher than the corresponding background

value of Hubei Province over the whole study area, but for Cr, the situation is opposite. Anyhow, Cd is strongly accumulated in soil and could be the largest soil pollution factor in Wuhan. In addition, the estimated results of RI and NPI indicate that almost the whole urban area of Wuhan is facing considerable potential ecological risk caused by soil trace metal pollution.

The research on soil trace metals in different functional zones reveals that Pb, Zn, Cu, and Cd have generally higher concentrations in roadsides, industrial areas, and residential areas than in school areas, greenbelts, and agricultural areas. Analysis of urbanization effect on trace metal accumulation shows that areas with higher road and population densities and longer urban construction history usually have higher trace metal concentrations. The above results indicate that vehicular emission, industrial activities, and household wastes may be the three main sources for trace metal accumulation in Wuhan, and increasing vegetation cover may reduce the threat of trace metals. Hot spot areas identified from the spatial distribution maps of the trace metals prove once again that trace metal accumulation is caused by the integrated effect of those three main sources.

In general, this study furthers our understanding of the environmental status in the urban area of Wuhan. It is suggested that effective measures should be taken to reduce trace metal contamination in urban soils to protect human health in this important large city.

Acknowledgments The research was supported by National Natural Science Foundation of China (Grant No. 41101193), and the Fundamental Research Funds for National Universities (Grant No. 2662014PY062). Opinions in the paper do not constitute an endorsement or approval by the funding agencies and only reflect the personal views of the authors.

Appendix 1: Data quality verification

A dataset of a previous study (Qu et al. 2014), kindly provided by Qu et al., was used for data quality verification of ICP-AES and XRF measurements in this paper. Considering the high spatial variability of trace metals, data points located within the Wuhan Donghu High-tech Development Park, which was the region of the previous study, were extracted. Concentrations of Pb, Zn, Cu, Cr, and Cd by ICP-AES and XRF in this paper were compared to the previous study based on the independent sample *t* test method. Results listed in Table 5 show that concentrations of Pb, Zn, and

Cr by ICP-AES and Pb and Zn by XRF in this study well match those in the previous study ($p > 0.05$), while concentrations of Cu and Cd by ICP-AES and Cr by XRF are significantly different from those in the previous study ($p < 0.05$). But, the range of Cd contents is comparable with results by Qu et al. (2013) and Yang et al. (2009). The above results indicate that concentrations of Pb, Zn, Cr, and Cd in this study could be trusted, while the significant difference between Cu contents in this study and the previous study may be caused by the high coefficient of variation of Cu (see the “Trace metal concentrations in urban soils” section).

Table 5 Summary statistics and results of two independent sample *t* tests of soil trace metal concentrations (mg/kg) by different methods

Element	Method	Minimum	Median	Maximum	Mean	SD	<i>t</i> tests <i>p</i>
Pb	XRF	13.93	21.71	88.63	23.88	10.32	0.847 ^a
	ICP-AES	11.97	22.04	36.31	22.21	5.14	0.931 ^a
	<i>ICP_Qu</i>	5.19	17.81	127.07	19.37	12.64	–
Zn	XRF	32.84	60.37	152.52	66.17	21.64	0.741 ^a
	ICP-AES	19.22	65.39	135.66	65.96	23.56	0.848 ^a
	<i>ICP_Qu</i>	23.18	56.55	180.73	61.2	23.86	–
Cu	XRF	26.27	35.14	54.70	36.01	7.07	0.000 ^b
	ICP-AES	0.24	6.19	34.66	8.88	7.43	0.000 ^b
	<i>ICP_Qu</i>	13.79	29.44	68.7	30.59	10.08	–
Cr	XRF	68.68	122.21	233.75	123.30	28.51	0.000 ^b
	ICP-AES	20.06	41.05	57.19	41.55	8.47	0.301 ^a
	<i>ICP_Qu</i>	1.14	35.89	102.34	38.8	17.02	–
Cd	XRF	–	–	–	–	–	–
	ICP-AES	1.02	3.04	4.58	3.01	0.87	0.000 ^b
	<i>ICP_Qu</i>	0.26	0.68	1.94	0.74	0.32	–

Superscript letter “a” means that trace metal concentrations are not significantly different from previous study ($p > 0.05$) and “b” trace metal concentrations are significantly different from previous study ($p < 0.05$). *ICP_Qu* refers to the dataset of previous study provided by Qu et al. (2014)

SD standard deviation

Appendix 2: XRF data transformation

To integrate trace metal data obtained by ICP-AES and XRF, regression models were established based on the pairwise concentrations of Pb, Zn, Cu, and Cr in the training samples (no Cd data by XRF).

Shown as Fig. 8, concentrations of Pb, Zn, and Cu obtained by XRF had significantly positive relationship

with the corresponding ICP-AES measurements; the coefficient of correlation were 0.915, 0.946, and 0.808 for Pb, Zn, and Cu, respectively. XRF measurements fitted fairly well with the ICP-AES measurements for Pb, Zn, and Cu, and the R^2 values were 0.842, 0.895, and 0.675, respectively. On the contrary, Cr by XRF showed no significant relationship with that by ICP-AES, with a quite

low R^2 value of 0.027. Wu et al. (2012) also found that XRF measurements of Pb, Zn, Ni, and Cu are highly reliable and agrees well with the ICP-AES experiments, while Cr and Cd by XRF show poor accuracy. Before transformation, BDLs of XRF were examined. A total of 107 BDLs for Pb, 2 BDLs for Zn, and 151 BDLs for Cu were excluded from the dataset. Since XRF-measured Cr was not accurate and no XRF measurement of Cd was higher than the detection limit, XRF measurements of Cr and Cd were abandoned and only ICP measurements of these two elements were used in further analysis. Although 50 % of the detection

limit may be used as the substitution in cases where concentrations were BDLs (Zibret 2012), taking this substitution into account would bring about big errors when establishing regression models and performing the transformations. Therefore, in the data transformation stage, ICP measurements of Pb, Zn, Cu, Cr, and Cd were reserved at the training sample points, and XRF measurements of Pb, Zn, and Cu that were higher than detection limit were transformed using the regression models at other data points. The distributions of available data points for Pb, Zn, Cu, Cr, and Cd can be found in Fig. 9.

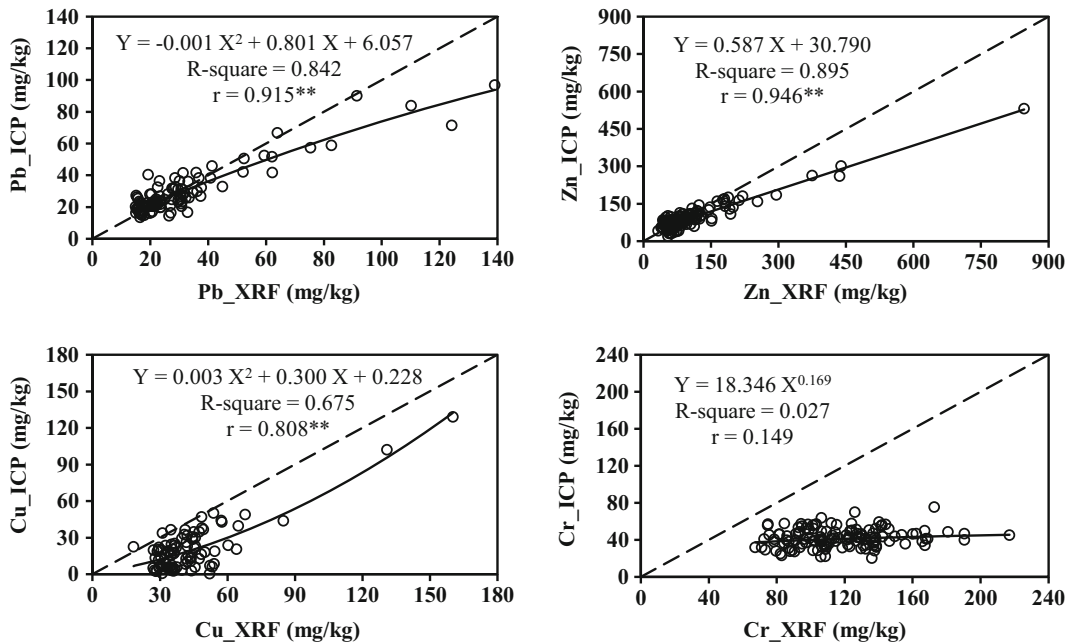


Fig. 8 Quantitative relationships between concentrations of Pb, Zn, Cu, and Cr (mg/kg) obtained by ICP-AES and XRF. *Dash lines* represent the 1:1 line and the *solid lines* represent the regression lines. Regression models, corresponding R^2 values, and coefficient of correlation are also presented in this figure

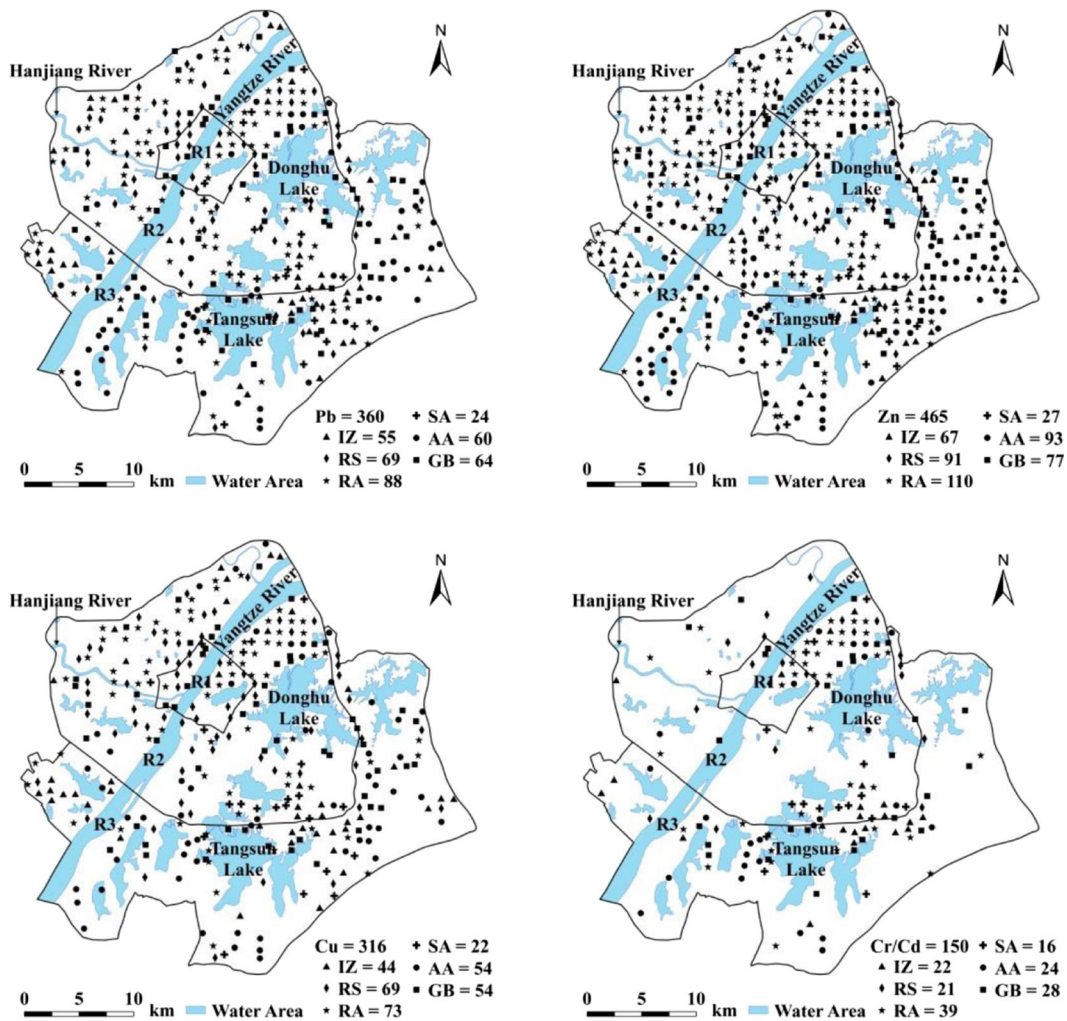


Fig. 9 Sampling sites used for analysis of Pb, Zn, Cu, Cr, and Cd. IZ, RS, RA, SA, AA, and GB refer to industrial zone, roadside, residential area, school area, agricultural area, and greenbelt,

respectively. The two black ring lines represent the 1st Ring Road and the 3rd Ring Road of Wuhan City, respectively

References

- Anikwe, M. A. N., & Nwobodo, K. C. A. (2002). Long term effect of municipal waste disposal on soil properties and productivity of sites used for urban agriculture in Abakaliki, Nigeria. *Bioresource Technology*, 83(3), 241–250. doi:10.1016/S0960-8524(01)00154-7.
- Atafar, Z., Mesdaghinia, A., Nouri, J., Homae, M., Yunesian, M., Ahmadimoghaddam, M., et al. (2010). Effect of fertilizer application on soil heavy metal concentration. *Environmental Monitoring and Assessment*, 160(1–4), 83–89. doi:10.1007/s10661-008-0659-x.
- Benhaddya, M., & Hadjel, M. (2014). Spatial distribution and contamination assessment of heavy metals in surface soils of Hassi Messaoud, Algeria. *Environmental Earth Sciences*, 71(3), 1473–1486. doi:10.1007/s12665-013-2552-3.
- Birke, M., & Rauch, U. (2000). Urban Geochemistry: Investigations in the Berlin Metropolitan Area. *Environmental Geochemistry and Health*, 22(3), 233–248. doi:10.1023/a:1026554308673.
- Bright, E. A., Rose, A. N., & Urban, M. L. (2013). LandScan 2013 Global Population Database. East View Information Services. O. R. N. Laboratory.
- Cai, Q. Y., Mo, C. H., Li, H. Q., Lü, H. X., Zeng, Q. Y., Li, Y. W., et al. (2013). Heavy metal contamination of urban soils and dusts in Guangzhou, South China. *Environmental Monitoring and Assessment*, 185(2), 1095–1106. doi:10.1007/s10661-012-2617-x.

- Chen, X. D., Lu, X. W., Li, L. Y., & Yang, G. (2013). Spatial distribution and contamination assessment of heavy metals in urban topsoil from inside the Xi'an second ringroad, NW China. *Environmental Earth Sciences*, 68(7), 1979–1988. doi:10.1007/s12665-012-1885-7.
- China National Environmental Monitoring Centre. (1990). *The background values of soil elements in China*. Beijing: China Environmental Science Press.
- Gong, M., Wu, L., Bi, X. Y., Ren, L. M., Wang, L., Ma, Z. D., et al. (2010). Assessing heavy-metal contamination and sources by GIS-based approach and multivariate analysis of urban–rural topsoils in Wuhan, central China. *Environmental Geochemistry and Health*, 32(1), 59–72.
- Guo, G. H., Wu, F. C., Xie, F. Z., & Zhang, R. Q. (2012). Spatial distribution and pollution assessment of heavy metals in urban soils from southwest China. *Journal of Environmental Sciences*, 24(3), 410–418. doi:10.1016/S1001-0742(11)60762-6.
- Gupta, S., Satpati, S., Nayek, S., & Garai, D. (2010). Effect of wastewater irrigation on vegetables in relation to bioaccumulation of heavy metals and biochemical changes. *Environmental Monitoring and Assessment*, 165(1–4), 169–177. doi:10.1007/s10661-009-0936-3.
- Hakanson, L. (1980). An ecological risk index for aquatic pollution control. a sedimentological approach. *Water Research*, 14(8), 975. doi:10.1016/0043-1354(80)90143-8.
- Helmreich, B., Hilliges, R., Schriewer, A., & Horn, H. (2010). Runoff pollutants of a highly trafficked urban road - correlation analysis and seasonal influences. *Chemosphere*, 80(9), 991–997. doi:10.1016/j.chemosphere.2010.05.037.
- Jiang, J. H., Xu, Y. H., & Peng, H. (2014). Distribution and speciation of heavy metals in sediments from Donghu Lake, Wuhan, China. *Fresenius Environmental Bulletin*, 23(2A), 502–507.
- Johansson, C., Norman, M., & Burman, L. (2009). Road traffic emission factors for heavy metals. *Atmospheric Environment*, 43(31), 4681–4688. doi:10.1016/j.atmosenv.2008.10.024.
- Lin, Y. P., Teng, T. P., & Chang, T. K. (2002). Multivariate analysis of soil heavy metal pollution and landscape pattern in Changhua county in Taiwan. *Landscape and Urban Planning*, 62(1), 19–35. doi:10.1016/S0169-2046(02)00094-4.
- Liu, H. L., Li, L. Q., Yin, C. Q., & Shan, B. Q. (2008). Fraction distribution and risk assessment of heavy metals in sediments of Moshui Lake. *Journal of Environmental Sciences*, 20(04), 390–397.
- Liu, C. L., Yu, R. L., & Duan, D. Z. (2014). Spatial-temporal structure of capacity fractal about urban–rural road network in Wuhan Metropolitan Area (in Chinese). *Geographical Research*, 33(4), 777–788.
- Ljung, K., Otabbong, E., & Selinus, O. (2006). Natural and anthropogenic metal inputs to soils in urban Uppsala, Sweden. *Environmental Geochemistry and Health*, 28(4), 353–364. doi:10.1007/s10653-005-9031-z.
- Ma, Z. D., Zhang, D. C., Bi, X. Y., Liu, G. Q., Ren, L. M., & Quan, H. L. (2005). Origin of cadmium high-value zones along the Yangtze River and Hanjiang River in Wuhan, Hubei, China (in Chinese). *Geological Bulletin of China*, 24(8), 740–743.
- Mahanta, M., & Bhattacharyya, K. (2011). Total concentrations, fractionation and mobility of heavy metals in soils of urban area of Guwahati, India. *Environmental Monitoring and Assessment*, 173(1–4), 221–240. doi:10.1007/s10661-010-1383-x.
- Meza-Figueroa, D., De la O-Villanueva, M., & De la Parra, M. L. (2007). Heavy metal distribution in dust from elementary schools in Hermosillo, Sonora, México. *Atmospheric Environment*, 41(2), 276–288. doi:10.1016/j.atmosenv.2006.08.034.
- Odewande, A., & Abimbola, A. (2008). Contamination indices and heavy metal concentrations in urban soil of Ibadan metropolis, southwestern Nigeria. *Environmental Geochemistry and Health*, 30(3), 243–254. doi:10.1007/s10653-007-9112-2.
- Peng, C., Ouyang, Z., Wang, M., Chen, W., Li, X., & Crittenden, J. C. (2013). Assessing the combined risks of PAHs and metals in urban soils by urbanization indicators. *Environmental Pollution*, 178, 426–432. doi:10.1016/j.envpol.2013.03.058.
- Qu, M. K., Li, W. D., Zhang, C. R., Wang, S. Q., Yang, Y., & He, L. Y. (2013). Source apportionment of heavy metals in soils using multivariate statistics and geostatistics. *Pedosphere*, 23(4), 437–444. doi:10.1016/S1002-0160(13)60036-3.
- Qu, M. K., Li, W. D., & Zhang, C. R. (2014). Spatial distribution and uncertainty assessment of potential ecological risks of heavy metals in soil using sequential gaussian simulation. *Human and Ecological Risk Assessment*, 20(3), 764–778. doi:10.1080/10807039.2013.770352.
- Rizo, O. D., Castillo, F. E., López, J. O. A., & Merlo, M. H. (2011). Assessment of heavy metal pollution in urban soils of Havana City, Cuba. *Bulletin of Environmental Contamination and Toxicology*, 87(6), 414–419. doi:10.1007/s00128-011-0378-9.
- Rose, N., Cowie, C., Gillett, R., & Marks, G. B. (2009). Weighted road density: A simple way of assigning traffic-related air pollution exposure. *Atmospheric Environment*, 43(32), 5009–5014. doi:10.1016/j.atmosenv.2009.06.049.
- Salonen, V.-P., & Korkka-Niemi, K. (2007). Influence of parent sediments on the concentration of heavy metals in urban and suburban soils in Turku, Finland. *Applied Geochemistry*, 22(5), 906–918. doi:10.1016/j.apgeochem.2007.02.003.
- Shi, G., Chen, Z., Xu, S., Zhang, J., Wang, L., Bi, C., et al. (2008). Potentially toxic metal contamination of urban soils and roadside dust in Shanghai, China. *Environmental Pollution*, 156(2), 251–260. doi:10.1016/j.envpol.2008.02.027.
- State Environmental Protection Administration of China (1995). Environmental quality standard for soils.
- Wei, B. G., Jiang, F. Q., Li, X. M., & Mu, S. Y. (2009). Spatial distribution and contamination assessment of heavy metals in urban road dusts from Urumqi, NW China. *Microchemical Journal*, 93(2), 147–152. doi:10.1016/j.microc.2009.06.001.
- Wu, C. M., Tsai, H. T., Yang, K. H., & Wen, J. C. (2012). How reliable is X-ray fluorescence (XRF) measurement for different metals in soil contamination? *Environmental Forensics*, 13(2), 110–121. doi:10.1080/15275922.2012.676603.
- Wuhan bureau of statistics. (2012). *2012 Wuhan statistical year-book*. Beijing: China Statistics Press.
- Wuhan bureau of statistics (2013). The Wuhan Statistical Bulletin of National Economic and Social Development. <http://www.whjt.gov.cn/details.aspx?id=2180>. Accessed 21 May 2014.
- Xia, X. H., Chen, X., Liu, R. M., & Liu, H. (2011). Heavy metals in urban soils with various types of land use in Beijing,

- China. *Journal of Hazardous Materials*, 186(2–3), 2043–2050. doi:10.1016/j.jhazmat.2010.12.104.
- Yang, Z. F., Wang, Y., Shen, Z. Y., Niu, J. F., & Tang, Z. W. (2009). Distribution and speciation of heavy metals in sediments from the mainstream, tributaries, and lakes of the Yangtze River catchment of Wuhan, China. *Journal of Hazardous Materials*, 166(2–3), 1186–1194. doi:10.1016/j.jhazmat.2008.12.034.
- Yang, X. F., Xiong, B. X., & Yang, M. S. (2010). Relationships among heavy metals and organic matter in sediment cores from Lake Nanhu, an Urban Lake in Wuhan, China. *Journal of Freshwater Ecology*, 25(2), 243–249. doi:10.1080/02705060.2010.9665074.
- Yang, T., Zeng, Q. L., Liu, Z. F., & Liu, Q. S. (2011). Magnetic properties of the road dusts from two parks in Wuhan city, China: implications for mapping urban environment. *Environmental Monitoring and Assessment*, 177(1–4), 637–648. doi:10.1007/s10661-010-1662-6.
- Yang, J., Meng, X. Z., Duan, Y. P., Liu, L. Z., Chen, L., & Cheng, H. F. (2014). Spatial distributions and sources of heavy metals in sediment from public park in Shanghai, the Yangtze River Delta. *Applied Geochemistry*, 44, 54–60. doi:10.1016/j.apgeochem.2013.08.007.
- Zhao, J. H., Li, H. Y., Gong, X., Du, W. M., & Hu, R. F. (2011). Study of soil organic carbon content in some typical functional areas, Wuhan City (in Chinese). *Journal of Anhui Agricultural Sciences*, 39(6), 3409–3410,3415.
- Zheng, N., Wang, Q. C., Zhang, X. W., Zheng, D. M., Zhang, Z. S., & Zhang, S. Q. (2007). Population health risk due to dietary intake of heavy metals in the industrial area of Huludao city, China. *Science of the Total Environment*, 387(1–3), 96–104. doi:10.1016/j.scitotenv.2007.07.044.
- Zibret, G. (2012). Impact of dust filter installation in ironworks and construction on brownfield area on the toxic metal concentration in street and house dust (Celje, Slovenia). *Ambio*, 41(3), 292–301. doi:10.1007/s13280-011-0188-7.